Journal of Power Sources 267 (2014) 491–502

Contents lists available at ScienceDirect

Journal of Power Sources

journal homepage: www.elsevier.com/locate/jpowsour

Optimal adaptation of equivalent factor of equivalent consumption minimization strategy for fuel cell hybrid electric vehicles under active state inequality constraints

Jihun Han [a], Youngjin Park [a], Dongsuk Kum [b, *]

[a] Department of Mechanical Engineering, Korea Advanced Institute of Science and Technology (KAIST), 291 Daehak-ro, Yuseong-gu, Daejeon 305-701, Republic of Korea
[b] The Cho Chun Shik Graduate School of Green Transportation, Korea Advanced Institute of Science and Technology (KAIST), 291 Daehak-ro, Yuseong-gu, Daejeon 305-701, Republic of Korea

HIGHLIGHTS

- We discuss DP, PMP, and ECMS in presence of state inequality constraints.
- We use DP solution for extracting optimal equivalent factor trajectory.
- Equivalent factor must be adjusted drastically if state constraints are active.
- Equivalent factor adaptation prevents loss of recuperation energy under downhill road.

ARTICLE INFO

Article history:
Received 5 March 2014
Received in revised form
11 May 2014
Accepted 12 May 2014
Available online 24 May 2014

Keywords:
Energy management strategy
Equivalent consumption minimization strategy
Equivalent factor adaptation
State inequality constraint
Dynamic programming
Fuel cell hybrid electric vehicle

ABSTRACT

Among existing energy management strategies (EMSs) for fuel cell hybrid electric vehicles (FCHEV), the equivalent consumption minimization strategy (ECMS) is often considered as a practical approach because it can be implemented in real-time, while achieving near-optimal performance. However, under real-world driving conditions with uncertainties such as hilly roads, both near-optimality and charge-sustenance of ECMS are not guaranteed unless the equivalent factor (EF) is optimally adjusted in real-time. In this paper, a methodology of extracting the globally optimal EF trajectory from dynamic programming (DP) solution is proposed for the design of EF adaptation strategies. In order to illustrate the performance and process of the extraction method, a FCHEV energy management problem under hilly road conditions is investigated as a case study. The main goal is to learn how EF should be adjusted and the impact of EF adaptation on fuel economy under several hilly road cases. Using the extraction method, the DP-based EF is computed, and its performance is compared with those of Pontryagin's minimum principle (PMP) and conventional ECMS. The results show that the optimal EF adaptation significantly improves fuel economy when the battery SoC constraint becomes active, and thus EF must be properly adjusted under severely hilly road conditions.

1. Introduction

Fuel cell technology is one of the promising long-term energy solutions for future transportation systems because it can eliminate tail-pipe CO_2 emissions as well as other harmful emissions. Generally, fuel cell-powered vehicles are equipped with an energy storage system and are often called fuel cell hybrid electric vehicle (FCHEV) because the addition of an energy storage system creates an additional degree of freedom in power flow. This allows the fuel cell system to operate more reliably and efficiently. For harnessing the full potential of FCHEVs, power coordination between the two energy sources, known as energy management strategy (EMS), is very important, and the optimal EMS has been studied widely over the past decade.

Existing EMSs can be classified into three types: rule-based approach, horizon optimization approach, and instantaneous (real-time) optimization approach. Rule-based approaches use a deterministic rule or a fuzzy set of rules, designed heuristically

* Corresponding author. Tel.: +82 42 350 1266; fax: +82 42 350 1250.
E-mail addresses: heylele@kaist.ac.kr (J. Han), yjpark@kaist.ac.kr (Y. Park), dskum@kaist.ac.kr (D. Kum).

http://dx.doi.org/10.1016/j.jpowsour.2014.05.067
0378-7753/

Nomenclature

BT	battery
DP	dynamic programming
ECMS	equivalent consumption minimization strategy
EF	equivalent factor
EMS	energy management strategy
FC	fuel cell
FCHEV	fuel cell hybrid electric vehicle
GPS	global positioning system
HEV	hybrid electric vehicle
HJB	Hamiltonian Jacobi Bellman
PMP	Pontryagin's minimum principle
SoC	state of charge in battery system

based on the efficiency of each power source [1,2]. Other recent studies attempt to optimize the performance of rule-based controllers by calibrating control parameters and thresholds that determine operation mode switching [3,4], but the optimization of multiple control parameters under real-world driving conditions with many uncertainties are challenging and their optimality are not guaranteed. In order to ensure the optimality, horizon optimization method such as Dynamic Programming (DP) is widely used [5,6]. However, DP cannot be implemented as a real-time controller because it requires complete driving cycle information a priori and imposes a heavy computational burden [7,8]. In contrast, instantaneous optimization methods such as equivalent consumption minimization strategy (ECMS) are easy to implement, but their global optimality over the horizon is not guaranteed [9]. However, it is widely accepted that ECMS achieves near-optimal performance with the selection of an appropriate equivalent factor (EF) [10–12]. A few studies have proposed a method for determining the EF using a pattern recognition algorithm for achieving near-optimal performance under real-world driving conditions [13].

The near-optimality of ECMS, however, no longer holds when state inequality constraints become active. For instance, when uncertainties such as a hilly road section are present, constant EFs cannot guarantee the charge-sustenance and near-optimality. For solving this problem, many studies have proposed adaptive-ECMS, wherein the EF is adjusted based on the battery state-of-charge (SoC) [14,15]. While these online adaptive ECMSs yield practical benefits in terms of charge sustenance, they do not guarantee near-optimality and even charge-sustenance under active state inequality constraints. In Ref. [16], a predictive reference signal generator was proposed for generating the desired battery SoC trajectory, which helps maximize energy recuperation under state inequality constraints. Although this approach helps recuperating a greater amount of braking energy while maintaining SoC within the admissible range as compared with the conventional ECMS, it cannot be considered as benchmark that guarantees global optimality.

A practical method of guaranteeing near-optimality would be to adjust EF using the horizon optimization approach. A means of obtaining a good reference EF trajectory is the use of Pontryagin's minimum principle (PMP) approach because the PMP necessary condition includes costate dynamics, which essentially represents the optimal EF trajectory [17,18]. In particular, for HEV applications, it is widely accepted that the PMP solution is unique and globally optimal [19]. However, under active state inequality constraints, PMP problem formulation is not trivial, and the solutions are no longer unique. There have been attempts to formulate and solve PMP problems with state inequality constraints. For instance, Kim et al. used an optimal control theory that converts the state inequality constraint into a new single equality constraint as a part of the necessary condition [19,21]. In addition, Kim et al. proposed the use of a jump condition, which allows discontinuity of the costate dynamics for plug-in HEV energy management problems [20]. However, these approaches lead to multiple local minimum solutions, and these solutions do not guarantee optimality unless many iterations are carried out for determining the globally optimal solution. Therefore, a methodology for extracting the globally optimal EF trajectory from the DP solution is proposed, including extreme case of active state inequality constraints. This method can potentially be used for designing an adaptive ECMS, the EF of which tries to mimic the EF extracted from DP solutions.

The main contributions of this paper are as follows: 1) The strengths and limitations of three EMSs (DP, PMP, and ECMS) under state inequality constraints are discussed. 2) A simple but effective method is proposed for extracting the globally optimal EF trajectory that preserves the state inequality constraints from DP solution. This method can provide valuable insights into how to adjust EF for achieving global optimal performance as a benchmark for online ECMS adaptation. 3) A case study is carried out for checking the DP-based EF trajectory corresponding to conditions in which hilly road conditions activates SoC constraints or not. The results show that when hilly road conditions activate SoC constraints, the loss of optimality of ECMS is significant, and thus the EF must be adjusted appropriately for achieving both near-optimal fuel economy and charge sustenance.

The remainder of this paper is organized as follows: Section 2 includes an introduction to the FCHEV system configuration and system modeling. Section 3 explains the horizon optimization approach under state inequality constraints. In Section 4, ECMS is addressed as one of the instantaneous optimization approaches. In the presence of state inequality constraints, the EF role of ECMS is emphasized for achieving charge sustenance and near-optimality. Therefore, the method to extract the optimal EF trajectory from the DP solution is introduced. Section 5 discusses a case study in which ECMS with DP-based EF is applied to a real-world driving condition. The results of the case study show that the DP-based EF trajectory provides a reference and valuable insights into how EF should be adjusted under hilly road conditions. Finally, in Section 6, the summary and conclusions of this study are presented.

2. FCHEV system configuration

In this section, a system-level FCHEV model is introduced for energy management studies. Fig. 1 shows a block diagram of the FCHEV model, which consists of a fuel cell system, battery system, and vehicle. The fuel cell system acts as the main electrical power source for the system bus, and the electrical power supplied by the battery is determined as follows.

$$P_{\text{demand}} = P_{\text{BT·req}} + P_{\text{FC·req}} \tag{1}$$

This power bus relationship is based on the fact that the two energy sources put together must provide the power required by a driving cycle.

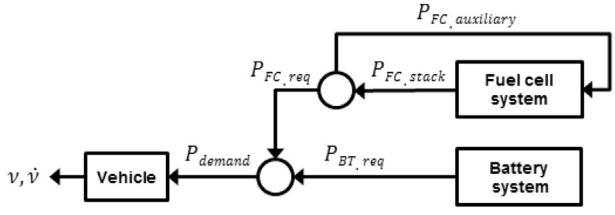

Fig. 1. Block diagram of FCHEV model.

In this study, system-level EMS is chosen, and a simplified FCHEV model is used. Furthermore, the efficiency map of electric motor and constant inverter efficiency are included for calculating electric power demand of the driving cycle. The target FCHEV is a sports utility vehicle, and its specifications are listed in Table 1.

2.1. Fuel cell system

The fuel cell system is the main power source in FCHEVs. It converts hydrogen into electrical energy through electrochemical reactions. In this study, a quasi-static FCHEV model is used for the fuel cell stack, which is widely accepted for system-level energy management problem formulation [22]. The fuel cell stack voltage is determined using a typical polarization curve, which is a function of current density.

The fuel cell system requires auxiliary systems that support the fuel cell stack. The auxiliary systems include a compressor, cooler, supply manifold, humidifier, and hydrogen circuit control system, and these systems consume electric power. Thus, the fuel cell stack must produce extra electric power for the auxiliary systems, and the total fuel cell stack power is given as follows:

$$P_{\mathrm{FC\cdot stack}} = P_{\mathrm{FC\cdot req}} + P_{\mathrm{FC\cdot auxiliary}} \tag{2}$$

Note that isothermal fuel cell stack operation is assumed.

If the required fuel cell stack power and fuel cell stack voltage are known, fuel cell current can be computed. Then, the hydrogen consumption rate is computed as follows:

$$\dot{m}_{\mathrm{H_2}} = N_{\mathrm{FC}} \cdot \frac{M_{\mathrm{H_2}}}{n_{\mathrm{e}} \cdot F} \cdot I_{\mathrm{FC}} \tag{3}$$

where N_{FC} denotes the number of cells in the fuel cell stack, $M_{\mathrm{H_2}}$ denotes the molar mass of hydrogen, n_{e} denotes the number of electrons, and F denotes Faraday's constant.

2.2. Battery system

The battery model was developed based on the simple resistive equivalent circuit model, where a voltage source, resistor, and the load are connected in series. The battery current is calculated from the requested battery power ($P_{\mathrm{BT,req}}$) as follows.

$$I_{\mathrm{BT}} = \frac{V_{\mathrm{BT\cdot OC}} - \sqrt{V_{\mathrm{BT\cdot OC}}^2 - 4 \cdot R_{\mathrm{BT\cdot int}} \cdot P_{\mathrm{BT\cdot req}}}}{2 \cdot R_{\mathrm{BT\cdot int}}} \tag{4}$$

where $V_{\mathrm{BT\cdot OC}}$ denotes open circuit voltage and $R_{\mathrm{BT\cdot int}}$ denotes internal resistance. Both open circuit voltage and internal resistance depend on the battery SoC. The Coulomb counting method, expressed using Eq. 5, is used for estimating SoC.

$$\mathrm{SoC}(t) = \mathrm{SoC}(t_0) - \frac{1}{Q_{\max}} \int_{t_0}^{t} I_{\mathrm{BT}}(t) dt \tag{5}$$

where $Q_{\max}$ denotes the maximum battery capacity.

Table 1
Vehicle specifications: sports utility vehicle (SUV).

Vehicle parameters	Value
Vehicle total mass	1936 kg
Front area	2.608 m^2
Air drag coefficient	0.44
Ambient air density	1.18 kg m^{-3}
Rolling resistance coefficient	0.013

2.3. Vehicle model

The force demand profile of a given driving cycle can be determined using the longitudinal vehicle dynamic model, which is mainly dependent on three force terms: rolling resistance, air drag resistance, and hill climbing resistance, as given by Eq. (6).

$$\begin{aligned} F_{\mathrm{demand}} &= m \cdot \dot{v} + F_{\mathrm{a}} + F_{\mathrm{r}} + F_{\mathrm{g}} \\ &= m \cdot \dot{v} + \frac{1}{2} \cdot \rho_{\mathrm{air}} \cdot A_{\mathrm{f}} \cdot c_{\mathrm{d}} \cdot v^2 + c_{\mathrm{r}} \cdot m \cdot g \cdot \cos(\alpha) + m \cdot g \cdot \sin(\alpha) \end{aligned} \tag{6}$$

where F_{a} denotes air drag resistance force, F_{r} denotes rolling resistance force, and F_{g} denotes climbing resistance force due to gravity on non-horizontal roads. v denotes vehicle speed, ρ_{air} denotes ambient air density, A_{f} denotes front area, C_{d} denotes air drag coefficient, C_{r} denotes rolling resistance coefficient, m denotes vehicle mass, g denotes acceleration due to gravity, and angle α denotes road slope.

3. Horizon optimization approach with state constraints

In this section, two popular horizon optimization methods, DP and PMP, are summarized and their strengths and limitations are discussed under active state inequality constraints. The optimal control problem is formulated as follows:

$$\text{Minimize } J = h\left(x\left(t_{\mathrm{f}}\right), t_{\mathrm{f}}\right) + \int_{t_0}^{t_f} g(x(t), u(t), \omega(t), t) dt \tag{7}$$

$$\text{Subject to } \dot{\mathbf{x}}(t) = \mathbf{f}(\mathbf{x}(t), \mathbf{u}(t), \boldsymbol{\omega}(t), t) \tag{8}$$

$$\mathbf{x}(t) \in \mathbf{X}(t), \mathbf{u}(t) \in \mathbf{U}(t) \tag{9}$$

where g is cost function, and h is the terminal state cost, which can be used for enforcing the final state constraint. x and u represent the state variable vector and the control input vector, respectively.

3.1. Dynamic programming (DP)

DP is a numerical method for solving multistage decision-making problems based on Bellman's principle of optimality [5,6]. The main strength of DP is that the globally optimal solution is guaranteed even for nonlinear non-convex problems with state and control constraints. However, DP suffers from heavy computational load and cannot be implemented in real-time controllers because all disturbances must be known a priori [18]. Thus, DP is often used as an optimal performance benchmark while designing a suboptimal real-time controller. For implementing DP, the original optimal control problem (Eqs. (7)–(9)) is discretized as follows.

$$\begin{aligned} &x_{k+1} = f_k(x_k, u_k, \omega_k), \quad k = 0, 1, \ldots, N-1, \\ &x_k \in X_k, \quad u_k \in U_k, \quad \omega_k \in W_k \end{aligned} \tag{10}$$

where state variables, control inputs, and disturbances are limited to subsets X_k, U_k, W_k, respectively.

Furthermore, the cost-to-go function from state x_k at time i to the final state x_N at time N is defined as follows:

$$J_k(x_k) = g_N(x_N) + \sum_{k=i}^{N-1} g_k(x_k, u_k, \omega_k) \tag{11}$$

where g_k indicates the incremental cost and g_N denotes the final cost, which includes additional cost of undesired final states.

By evaluating the cost-to-go backwards in time, the optimal control policy π^O that satisfies the following can be found.

$$\pi_k^O = \arg J_k^O(x_k)$$
$$\text{where } J_k^O(x_k) = \min_{u_k \in U_k} \left\{ g_k(x_k, u_k, \omega_k) + J_{k+1}^O(f_k(x_k, u_k, \omega_k)) \right\} \tag{12}$$

For the DP realization of FCHEVs, cost function, state, and control input are defined by fuel consumption (hydrogen mass flow rate), the battery SoC, and fuel cell power, respectively.

$$g = \dot{m}_{H_2}, \quad u = P_{FC\cdot req}, \quad x_1 = \text{SoC} \tag{13}$$

Furthermore, time grid is fixed to 1s, SoC grid is fixed to 0.5%, and $P_{FC.req}$ grid is fixed to 50 W. Namely, state variable SoC is quantized into 121 possible values with state inequality constraints $20\% \le x(k) \le 80\%$, control input $P_{FC.req}$ is quantized into 1501 possible values with control input inequality constraints $0 \le u(k) \le 75$ kW. For a more detailed description of the DP algorithm, see Ref. [23].

3.2. Pontryagin's minimum principle (PMP)

PMP is another horizon optimization method that was developed based on the calculus of variations. PMP solves the optimal control problem analytically with a considerably lower computational burden and is often considered as a DP alternative [19]. Although there may exist multiple local minimum solutions in the PMP approach, there exists a unique globally optimal solution for convex problems [19]. Furthermore, PMP can be derived from DP in continuous time under no state constraints (See Appendix). However, the handling of state inequality constraints within PMP is nontrivial. In this section, a simple method that can handle state inequality constraints as a part of the necessary conditions is introduced. This method converts all state inequality constraints into a single equality constraint by defining a new variable; then, the Hamiltonian function is augmented with this equality constraint [19,21]. If the number of state inequality constraints is l, ith state inequality constraint is described in following form:

$$h_i(\mathbf{x}(t), t) \ge 0, \quad i = 1, 2 \cdots, l \tag{14}$$

where h indicates each state inequality constraint defined by a function of state and time, and it has continuous first and second partial derivatives with respect to $x(t)$.

For handling l state inequality constraints together, a single equality constraint is newly defined as a new dynamic state variable x_{n+1}, as follows:

$$f_{n+1}(t) = \dot{x}_{n+1}(t) = \sum_{i=1}^{l} [h_i(x(t), t)]^2 \cdot \theta(-h_i),$$
$$\text{where } \theta(-h_i) = \begin{cases} 0, & h_i \ge 0 \\ 1, & h_i < 0 \end{cases} \tag{15}$$

where θ denotes the Heaviside step function.

The new equality constraint f_{n+1} is non-negative at all times and equals to zero only if all state inequality constraints are inactive. In other words, the Heaviside step function and the augmented equality constraint are active only when the state inequality constraints are active. The Hamiltonian function is augmented by the additional equality constraint with a new Lagrange multiplier, as expressed below:

$$H_n(\mathbf{x}, \mathbf{u}, \boldsymbol{\omega}, \boldsymbol{\lambda}, t) = g(\mathbf{x}, \mathbf{u}, \boldsymbol{\omega}, t) + \boldsymbol{\lambda}^T(t)\mathbf{f}(\mathbf{x}, \mathbf{u}, \boldsymbol{\omega}, t) + \lambda_{n+1}(t) f_{n+1}(\mathbf{x}, \mathbf{u}, \boldsymbol{\omega}, t) \tag{16}$$

The necessary conditions considering state constraints can now be derived from the augmented Hamiltonian function. Those that satisfy Eqs. (7)–(9) and Eqs. 14 and 15 are as follows:

$$\dot{\mathbf{x}}(t) = \left(\frac{\partial H_n(\mathbf{x}, \mathbf{u}, \boldsymbol{\omega}, \boldsymbol{\lambda}, t)}{\partial \boldsymbol{\lambda}} \right)^T = \mathbf{f}(\mathbf{x}, \mathbf{u}, \boldsymbol{\omega}, t)$$
$$\dot{x}_{n+1}(t) = \frac{\partial H_n(\mathbf{x}, \mathbf{u}, \boldsymbol{\omega}, \boldsymbol{\lambda}, t)}{\partial \lambda_{n+1}} = f_{n+1}(\mathbf{x}, \mathbf{u}, \boldsymbol{\omega}, t) \tag{17}$$

$$\dot{\boldsymbol{\lambda}}(t) = -\left(\frac{\partial H_n(\mathbf{x}, \mathbf{u}, \boldsymbol{\omega}, \boldsymbol{\lambda}, t)}{\partial \mathbf{x}} \right)^T = -\left(\frac{\partial g(\mathbf{x}, \mathbf{u}, \boldsymbol{\omega}, t)}{\partial \mathbf{x}} \right)^T - \left(\frac{\partial \mathbf{f}(\mathbf{x}, \mathbf{u}, \boldsymbol{\omega}, t)}{\partial \mathbf{x}} \right)^T \boldsymbol{\lambda}(t) - \left(\frac{\partial f_{n+1}(\mathbf{x}, \mathbf{u}, \boldsymbol{\omega}, t)}{\partial \mathbf{x}} \right)^T \lambda_{n+1}(t)$$
$$\dot{\lambda}_{n+1}(t) = -\frac{\partial H_n(\mathbf{x}, \mathbf{u}, \boldsymbol{\omega}, \boldsymbol{\lambda}, t)}{\partial x_{n+1}} = 0 \tag{18}$$

$$H_n(\mathbf{x}^*, \mathbf{u}^*, \boldsymbol{\omega}, \boldsymbol{\lambda}^*, t) \le H_n(\mathbf{x}^*, \mathbf{u}, \boldsymbol{\omega}, \boldsymbol{\lambda}^*, t) \text{ for all admissible } u(t) \tag{19}$$

where the dynamics of the new Lagrange multiplier is zero because the new state variable $x_{n+1}(t)$ does not explicitly depend on the new Hamiltonian function. If the final states and the final time are specified, the boundary conditions for the necessary conditions can be expressed as follows:

$$\mathbf{x}^*(t_0) = \mathbf{x}^*\left(t_f\right) = \mathbf{x}_0, \quad x_{n+1}^*(t_0) = 0, \quad x_{n+1}^*\left(t_f\right) = 0 \tag{20}$$

For the PMP realization of FCHEVs, the definitions of cost function, state, and control input are identical to those in Section 3.1. State inequality constraints denote admissible SoC range, thus, the new dynamic state variable for handling state inequality constraints is defined by h_1, h_2 as follows:

$$f_2 = \dot{x}_2 = h_1^2 \cdot \theta(-h_1) + h_2^2 \cdot \theta(-h_2)$$
$$\text{where } h_1 = x_1 - x_{\min} \ge 0, \quad h_2 = x_{\max} - x_1 \ge 0 \tag{21}$$

where h_1 represents the minimum SoC bound, and h_2 represents maximum SoC bound.

A new Lagrange multiplier λ_2 is employed to augment Hamiltonian function with new dynamic state variable as follows:

$$H_n = \dot{m}_{H_2} + \lambda_1 \cdot \dot{x}_1 + \lambda_2 \cdot \dot{x}_2 \tag{22}$$

From the PMP necessary conditions, the dynamics of the new Lagrange multiplier can be described as follows:

$$\dot{\lambda}_2(t) = -\frac{\partial H_n}{\partial x_2} = 0 \tag{23}$$

4. Instantaneous optimization approach with state constraints

4.1. Equivalent consumption minimization strategy (ECMS)

In this section, the strengths and limitations of the ECMS are described. Then, a simple adaptive ECMS considering state constraints is developed as a baseline real-time controller.

4.1.1. ECMS concept: role of equivalent factor

ECMS is an instantaneous optimization method that can be implemented as a real-time controller because its solution does not require future driving cycle information. It generates near-optimal performance when state constraints are inactive. For FCHEVs, the main concept of ECMS is that battery energy consumption is considered as future hydrogen consumption, and the total hydrogen consumption rate can be defined as follows.

$$\dot{m}_{\mathrm{eqv.}} = \dot{m}_{\mathrm{H_2}} + \dot{m}_{\mathrm{equi\cdot H_2\cdot by\cdot BT}} = \dot{m}_{\mathrm{H_2}} + \frac{s}{\mathrm{LHV_{H_2}}} P_{\mathrm{eBT}} \tag{24}$$

where $\dot{m}_{\mathrm{equi\cdot H_2\cdot by\cdot BT}}$ is the equivalent H_2 consumption rate from the battery, which can be obtained by using EF, s, lower heating value of H_2, $\mathrm{LHV_{H_2}}$, and the electric battery power, flow P_{eBT}.

For a given EF or s, the optimal power split ratio between the fuel cell system and battery can be computed. Then, the question becomes how to find the optimal EF that achieves charge sustenance without violating state and control constraints. One method of finding the optimal EF trajectory is using the PMP approach because the costate dynamics of the necessary condition represents the optimal EF trajectory. When state constraints are inactive (i.e., the battery SoC stays within the admissible SoC range), costate variation is relatively small. In this case, the PMP solution approaches ECMS with a constant EF, and the near-optimal ECMS performance is guaranteed. This necessitates computation of the constant optimal EF of ECMS that ensures charge sustenance over a given driving cycle. However, when the state constraints are active, the near-optimality of ECMS no longer holds. In fact, the constant EF that achieves charge sustenance in the absence of constraints suffers from a severe loss of optimality [16]. Therefore, the optimal EF must be adjusted appropriately for achieving near-optimal performance under active state constraints. For instance, when approaching a downhill section, the EF should be decreased to promote battery discharge before said section arrives for maximizing the recuperation of potential energy from the downhill section. Moreover, when a small battery is used for cost-, weight-, and volume reduction, the state constraints are activated easily, and, thus, the role of EF adaptation gains considerable importance.

4.1.2. ECMS with state constraints

In this section, a simple adaptive ECMS that can avoid the violation of state constraints is introduced as a baseline real-time controller ("conventional ECMS"). The conventional ECMS prevents violation of the state constraints by simply adding a penalty function to the constant EF, as expressed below.

$$s(t) = s + f_{\mathrm{p}}(t) \;\; \text{where,} \; f_{\mathrm{p}}(t) = \begin{cases} k_{\mathrm{p}}(x_{\max} - x) & x > x_{\max} \\ 0 & x_{\min} < x < x_{\max} \\ k_{\mathrm{p}}(x - x_{\min}) & x < x_{\min} \end{cases} \tag{25}$$

When the state approaches the boundary, the penalty function is activated for preventing the battery SoC from exceeding the SoC boundary. More specifically, if the battery SoC exceeds the maximum/minimum SoC bound, the penalty function decreases/increases EF to promote battery discharging/charging. In addition, when the SoC reaches the maximum SoC bound during braking, conventional mechanical braking is used instead of regenerative braking for preventing overcharging. Again, the reference EF value that ensures charge sustenance still needs to be computed through iterative search.

4.2. DP-based equivalent factor extraction method

In the literature, DP solution has been mainly used in two ways: 1) as a reference for evaluating the performance limit of a given design or the degree of optimality of proposed real-time controllers and 2) as a guideline for designing near-optimal rule-based controllers [24–27]. For instance, Kum et al. proposed a technique for extracting implementable control strategies that can be embedded into a rule-based controller [26,27]. The present study follows a similar approach for extracting optimal EF trajectory.

In this section, two methodologies of extracting the optimal EF trajectory that can be used as a benchmark for designing an EF adaptation law are presented; the first one is an analytical approach based on solving ECMS optimization problem under a few simplifying assumptions, and the second one is a numerical approach based on ECMS database. The main concepts of both approaches are to utilize DP results for determining optimal EF that leads ECMS to generate the same DP results. For the given battery SoC and power demand, there is a one-to-one relationship between EF and optimal fuel cell power computed by ECMS. Thus, specific EF value corresponding to DP results can be determined through inverse operation, as expressed below.

$$P^{*}_{\mathrm{FC}} = f(\mathrm{SoC}, P_{\mathrm{demand}}, s) \underset{f^{-1}}{\longrightarrow} s = f(\mathrm{SoC_{DP}}, P_{\mathrm{demand}}, P_{\mathrm{FC\cdot DP}}) \tag{26}$$

The proposed method is a simple, yet effective tool for ECMS-based EMS design because it provides many useful insights into EF adjustment under real-world driving conditions (e.g., drive pattern changes or hill road approaching). Eventually, it will act as a guideline for engineers designing EF adaptation laws that can achieve near-optimal performance while satisfying the battery charge sustenance requirement.

4.2.1. Analytical approach

If there are no bounds on states and control inputs, PMP can be derived from the Hamiltonian–Jacobi–Bellman (HJB) equation, and thus, the optimal costate trajectory equals the optimal cost function gradient, as described in the Appendix. However, when the state and control constraints are present, this equality no longer holds, and the analytical approach using HJB equation cannot be used to compute the optimal costate trajectory. Therefore, by solving ECMS optimization problem, derivation of EF formula that leads ECMS to generate DP results is emphasized. At first, the fuel cell and the battery models are simplified to define a quadratic cost function because an optimization problem with a quadratic cost function can be analytically solved. Then, the necessary and sufficient conditions for a minimum are solved to derive the analytic expression of optimal EF using DP results.

4.2.1.1. Model simplification

A. Simplified fuel cell model

Assuming that the fuel cell stack is not operated at low currents, the linear polarization curve is used so that the fuel cell voltage can be computed as a function of fuel cell current as shown below:

$$V_{\mathrm{FC}} = V_{\mathrm{FC\cdot OC}} - R_{\mathrm{FC}} I_{\mathrm{FC}} \tag{27}$$

where $V_{\mathrm{FC.OC}}$ denotes the voltage at a fuel cell current of zero (no-current state), and R_{FC} denotes the overall fuel cell resistance in the Ohmic loss region of the polarization curve.

Assuming a linear polarization curve and negligible auxiliary power, the fuel cell current can be described as a function of fuel cell power. Then, the hydrogen mass flow rate can be expressed as

quadratic function of fuel cell power by taking Taylor's series approximation at $P_{FC,req} = 0$ as shown below:

$$\dot{m}_{H_2} = N_{FC}\frac{M_{H_2}}{n_e F} I_{FC} = N_{FC}\frac{M_{H_2}}{n_e F}\frac{V_{FC\cdot OC} - \sqrt{V_{FC\cdot OC}^2 - 4R_{FC}P_{FC\cdot req}}}{2R_{FC}}$$
$$\approx N_{FC}\frac{M_{H_2}}{n_e F}\left\{\frac{1}{V_{FC\cdot OC}}P_{FC\cdot req} + \frac{R_{FC}}{V_{FC\cdot OC}^3}P_{FC\cdot req}^2\right\} \quad (28)$$

B. Simplified battery model

Assuming the battery model as the simple resistive equivalent circuit model, the battery power loss is expressed as a function of battery power using Ohm's law, and then, approximated in the same way as in the previous section:

$$P_{BT\cdot loss} = R_{BT}I_{BT}^2 = \frac{\left(V_{BT\cdot OC} - \sqrt{V_{BT\cdot OC}^2 - 4R_{BT}P_{BT\cdot req}}\right)^2}{4R_{BT}} \approx \frac{R_{BT}}{V_{BT\cdot OC}^2}P_{BT\cdot req}^2 \quad (29)$$

4.2.1.2. ECMS cost function using simplified models. For solving an ECMS optimization problem analytically, it is necessary to change original cost function used in ECMS to quadratic cost function using simplified models. ECMS cost function representing equivalent fuel consumption can be modified as quadratic function of fuel cell power, as expressed in Eq. (30).

$$g_{ECMS} = \overbrace{\dot{m}_{H_2}\cdot LHV_{H_2}}^{P_{H_2}} + s\cdot\overbrace{(P_{BT} + P_{BT\cdot loss})}^{P_{eBT}} = N_{FC}\cdot\frac{M_{H_2}}{n_e F}\cdot LHV_{H_2}\cdot\left\{\frac{1}{V_{FC\cdot OC}}P_{FC} + \frac{R_{FC}}{V_{FC\cdot OC}^3}P_{FC\cdot req}^2\right\} + s\cdot\left(P_{BT} + \frac{R_{BT}}{V_{BT\cdot OC}^2}P_{BT\cdot req}^2\right)$$
$$= \mu_1 P_{FC\cdot req} + \mu_2 P_{FC\cdot req}^2 + s\cdot P_{BT\cdot req} + s\cdot\mu_3 P_{BT\cdot req}^2$$
$$= \mu_1 P_{FC\cdot req} + \mu_2 P_{FC\cdot req}^2 + s\cdot(P_{demand} - P_{FC\cdot req}) + s\cdot\mu_3(P_{demand} - P_{FC\cdot req})^2$$
$$= (s\mu_3 + \mu_2)\cdot P_{FC\cdot req}^2 + (\mu_1 - 2s\mu_3 P_{demand} - s)\cdot P_{FC\cdot req} + \left(sP_{demand} + s\mu_3 P_{demand}^2\right)$$
$$\text{where } \mu_1 = \frac{N_{FC}\cdot M_{H_2}\cdot LHV_{H_2}}{n_e\cdot F\cdot V_{FC\cdot OC}},\ \mu_2 = \frac{N_{FC}\cdot M_{H_2}\cdot LHV_{H_2}\cdot R_{FC}}{n_e\cdot F\cdot V_{FC\cdot OC}^3},\ \mu_3 = \frac{R_{BT}}{V_{BT\cdot OC}^2} \quad (30)$$

where, fuel cell power $P_{FC,req}$ is defined as the control input. Two power sources must provide power demand: $P_{demand} = P_{FC\cdot req} + P_{BT\cdot req}$.

4.2.1.3. Derivation of EF formula using necessary and sufficient conditions. The proposed method utilizes all of the optimal solution obtained from DP, which includes the battery SoC, fuel cell power, and power demand. As explained in Section 3.1, the battery SoC and fuel cell power computed from DP stay within the admissible state and control input range, respectively. Therefore, this problem is treated as an unconstrained optimization problem with ECMS cost function, and use necessary and sufficient conditions for a minimum cost function to derive the optimal EF formula. Second-order partial derivative of the ECMS cost function (the sufficient condition) is derived to distinguish between a minimum and a maximum, as follows:

$$\frac{\partial^2 g_{ECMS}}{\partial P_{FC\cdot req}^2} = 2(\mu_2 + s\mu_3) > 0 \quad (31)$$

Since the model parameters of power sources such as μ_2,μ_3 and s are always positive, quadratic cost function must have a minimum. The necessary condition for the solution to be the minimum is that the first-order partial derivative of the ECMS cost function must be zero. Using this necessary condition, the analytic expression of EF can be derived as shown below.

$$\frac{\partial g_{ECMS}}{\partial P_{FC\cdot req}} = 0 \Rightarrow s_{DP} = \frac{\mu_1 + 2\mu_2 P_{FC\cdot DP}}{1 + 2\mu_3(P_{demand} - P_{FC\cdot DP})} \quad (32)$$

For extracting globally optimal EF trajectory, this simple analytic EF formula can be used to compute EF based on DP results without ECMS database built a priori. For this reason, this algorithm is computationally efficient. Furthermore, since this formula is defined by parameters of power sources, parameters can be easily adjusted when the characteristics of models change.

4.2.2. Numerical (map-based) approach

If ECMS is implemented with EF trajectory obtained from the analytical approach introduced in the previous section, ECMS and DP results show similar trends in power distribution between the two power sources. However, they are not identical due to modeling errors. Therefore, from the practicality viewpoint, the numerical (map-based) approach based on ECMS database is presented. Overall Procedure is illustrated in Fig. 2. First, ECMS database is built by iterative optimization process. Then, DP results are computed by DP algorithm. Optimal EF trajectory is extracted from ECMS database and DP results through the inverse operation introduced in Eq. (26).

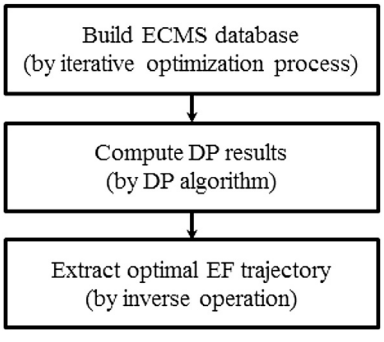

Fig. 2. Numerical approach procedure.

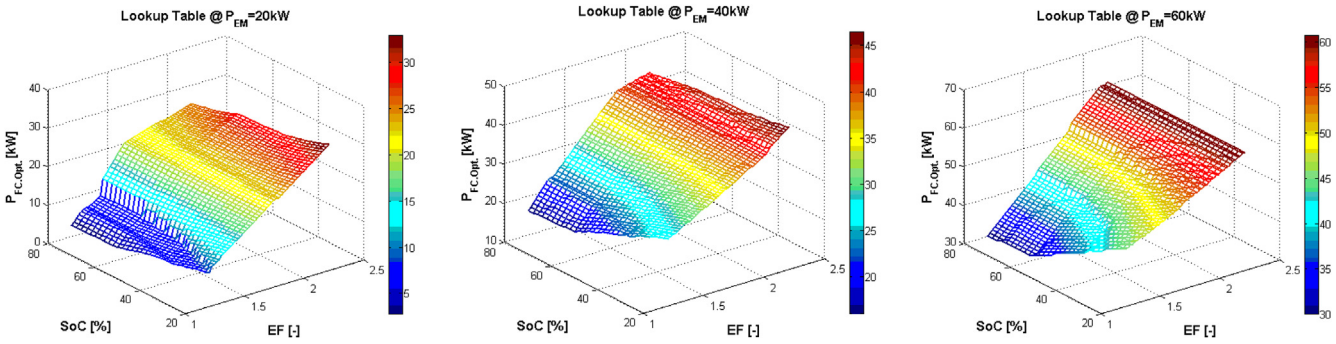

Fig. 3. ECMS database: optimal ECMS fuel cell power as a function of the battery SoC, power demand, and EF.

Respective static efficiency maps of the battery and fuel cell system are used to define nonlinear ECMS cost function, as expressed in Eq. (33). For given power demand, the battery SoC, iterative optimization process using this cost function is carried out for computing optimal fuel cell power. Then, computed value is stored in ECMS database as a map function of three variables; the battery SoC, power demand, and EF, as Fig. 3 shows.

$$g_{\mathrm{ECMS}} = \overbrace{\dot{m}_{\mathrm{H_2}} \cdot \mathrm{LHV}_{\mathrm{H_2}}}^{P_{\mathrm{H_2}}} + s \cdot \overbrace{\left(P_{\mathrm{BT}} + P_{\mathrm{BT\cdot loss}}\right)}^{P_{\mathrm{eBT}}} = \frac{P_{\mathrm{FC\cdot req}}}{\eta_{\mathrm{H_2}}\left(P_{\mathrm{FC\cdot req}}\right)} + s \cdot \frac{P_{\mathrm{BT\cdot req}}}{\eta_{\mathrm{BT}}\left(P_{\mathrm{BT\cdot req}}, \mathrm{SoC}\right)} \tag{33}$$

where, $\eta_{\mathrm{H_2}}$ is total fuel cell system efficiency, and η_{BT} is total battery system efficiency.

As in the previous section, DP results are also gathered and used to make the inverse operation to extract optimal EF. In ECMS database, for given the power demand and the battery SoC, optimal ECMS fuel cell power and EF also have one-to-one relationship. As last step of numerical (map-based) approach, therefore, EF corresponding to optimal fuel cell power obtained from DP can be searched in ECMS database.

In this study, the numerical (map-based) approach is chosen to analyze how to adjust EF corresponding to real-world driving conditions, as a part of designing adaptation laws for real-time ECMSs when the battery SoC violates its maximum/minimum bound; we call the ECMS with DP-based EF as DP-based ECMS. For example, when the FCHEV is driving on a hilly road, future driving information such as altitude profile should be used to properly adjust the EF for optimal performance. The influence of altitude profile on the general trend of DP-based ECMS is investigated in depth in a case study described in Section 5.

5. Case study: FCHEV control on hilly roads

This section consists of two parts: 1) offline study on three EMSs (DP-based ECMS, PMP, and conventional ECMS) and the optimal EF adjustment under two hilly road conditions; and 2) the evaluation of real-time EF adaptation law designed on the basis of DP-based EF results.

5.1. Study on the optimal EF adjustment under two hilly conditions

Two goals of this subsection are as follows: first one is comparative study on the performance of three EMSs corresponding to hilly roads, and the second one is analysis on how altitude profile influences EF trajectory for achieving the global optimality while satisfying the battery charge-sustenance.

5.1.1. Simulation environment

Two case studies, a downhill road with a slight grade and a downhill road with a steep grade, have been demonstrated in order to emphasize the impact of active state constraints on the needs for EF adjustments. Furthermore, these case studies provide insights on how EF should be adjusted for the optimal fuel economy when SoC constraints are activated by the hilly road.

The simulation test cycle was modified with the addition of the road grade profile to a US Federal Test Procedure (FTP)-highway driving cycle. The velocity profiles are assumed to be the same on two hilly roads. As shown in Fig. 4, the driver power demand is offset by negative power demands due to reduced demand when downhill road grades are present; the first slight downhill road is set to −10 kW (roughly −1.4°), and the second steep downhill road is set to −26.6 kW (roughly −3.7°).

The maximum SoC bound is set to 80%, minimum SoC bound is set to 20%, and initial battery SoC is set to 50%. Namely, the admissible SoC range is set to 20%–80% in order to ensure a long battery cycle-life while maintaining sufficient battery capacity for the recuperation of braking energy. When the SoC reaches the maximum SoC bound during braking, the supervisory controller switches from regenerative braking into conventional mechanical braking to prevent overcharging.

Suppose that future driving information can be known a priori, where offline iterative search determines the initial values of EF and costates of conventional ECMS and PMP for satisfying the battery SoC boundary condition, respectively. Then, the comparative analysis of three EMSs for two hilly road conditions is performed as follows.

5.1.2. First case: light downhill road

First case of hilly road with a slight grade represents the normal driving conditions when a hilly road profile does not lead the battery SoC to violate any SoC bound. In Fig. 5, the blue line represents DP-based ECMS (ECMS using DP-based EF; see Section

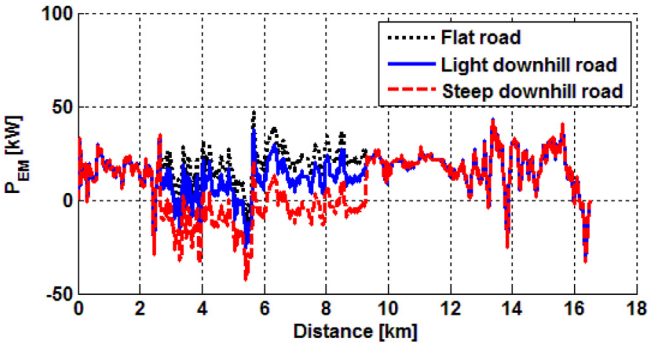

Fig. 4. Power demand profile corresponding to different hilly road.

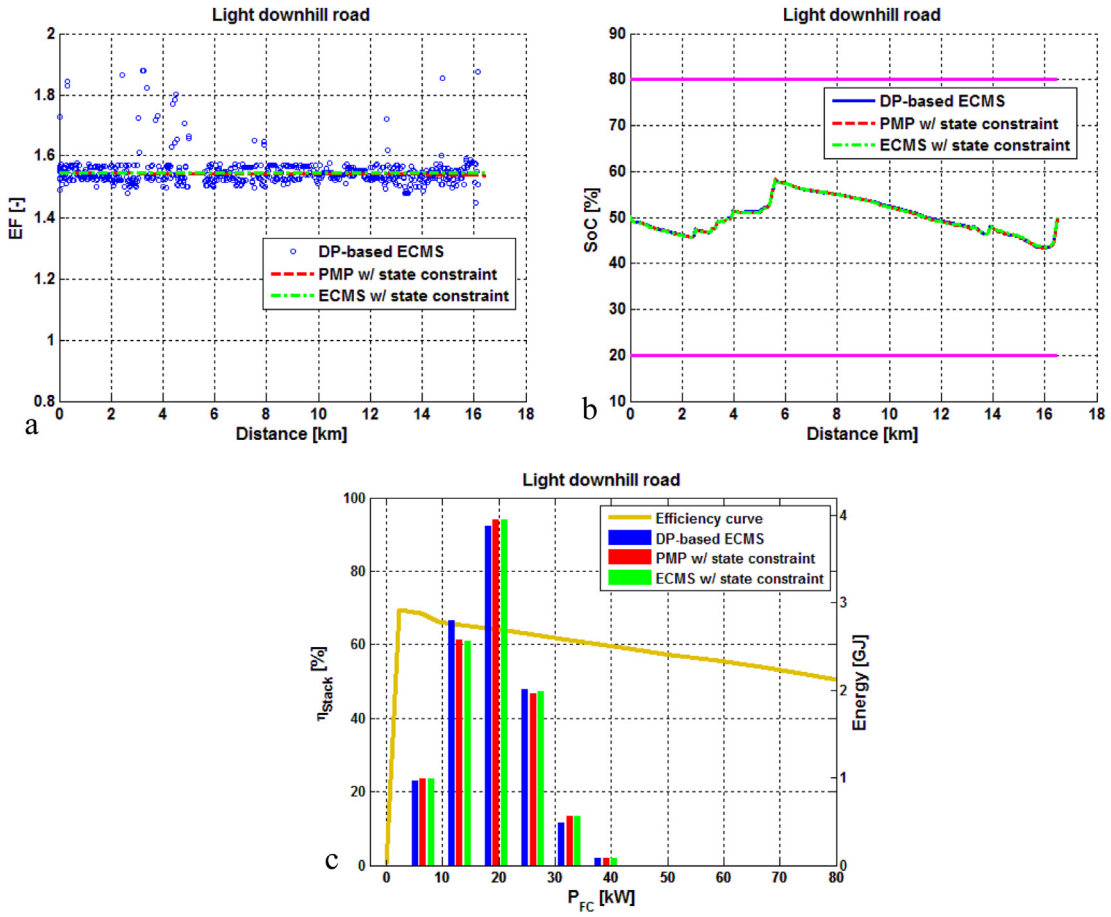

Fig. 5. First light downhill road for three EMSs (DP-based ECMS, PMP, conventional ECMS): (a) EF trajectory (b) battery SoC trajectory (c) energy histogram of fuel cell system. (For interpretation of the references to color in this figure legend, the reader is referred to the web version of this article.)

4.2.2), red dotted line represents PMP (see Section 3.2), and the green dash-dot represents conventional ECMS (see Section 4.1.2). All EMSs have the same constant EF value (or costate) because the variations in road slope are not large enough to activate the state constraints in Fig. 5(a). Note that the costate dynamics of PMP can be neglected under inactive state constraints. Furthermore, they generate the same SoC trajectory within the admissible SoC range (Fig. 5(b)). For this reason, the distribution of fuel cell power remains unchanged with various EMSs as shown in Fig. 5(c). Therefore, under a light downhill road condition, state constraints are no activated, and thus all EMSs achieve near-optimality and charge-sustenance using constant EF (costate).

5.1.3. Second case: steep downhill road

Second case for a steep downhill road represents an extreme driving condition in which hilly road profile activates the state constraints. As shown in Fig. 6(a), constant EF (costate) no longer works, and EF needs to be properly adjusted to maximize fuel economy while maintaining charge-sustenance. In particular, large deviations of SoC and EF trajectories between conventional ECMS, PMP, and the DP-based ECMS are observed. Since the penalty function of conventional ECMS is activated when the battery SoC reaches SoC bounds, it cannot prepare for the upcoming hilly road in advance, and thus a part of the recoverable braking energy is lost (Fig. 6(b). Consequently, the fuel cell must produce more energy to compensate for this lost energy, which leads to the loss of optimality and fuel economy. As shown in Figs. 6(c) and 7, fuel cell system of conventional ECMS operates more often at medium power range (20 kW–30 kW), and hydrogen consumption increases in comparison with other two EMSs. In contrast, other two EMSs discharge the battery to the minimum SoC bound before arriving at the downhill section. Namely, if potential energy of an upcoming hilly road is large enough to violate the maximum/minimum SoC bound, EF should be adjusted accordingly before driving into a hilly section.

Since the first PMP costate equation changes dramatically under active state constraints, the fuel economy and EF trajectory of PMP are very similar to those of the DP-based ECMS, which is the global optimal solution. However, PMP only provides the necessary conditions for optimal solutions and has multiple local minimum when the state constraints are active. Among them, the best solution that gives global minimum hydrogen consumption is chosen, and it is used for final comparison in Figs. 6 and 7. As Fig. 8 and Table 2 show, there exist many PMP cases which have local minimum. Note that iterative optimization process is needed to find initial costates which leads to one of the multiple local minimum. For this reason, the procedure of PMP for finding global minimum is inconvenient and time consuming. Conclusively, DP-based EF computed from the proposed method is considered as promising benchmark for design of adaptation law corresponding to various hilly road conditions.

5.2. Development of a real-time EF adaptation strategy for hilly roads

5.2.1. DP-based EF trajectory analysis

In addition to the two hilly road conditions described in Section 5.1.1, a medium downhill road is supplemented to obtain more detailed trends on how DP-based EF trajectories vary over several hilly road conditions. The medium downhill road is set to −20 kW

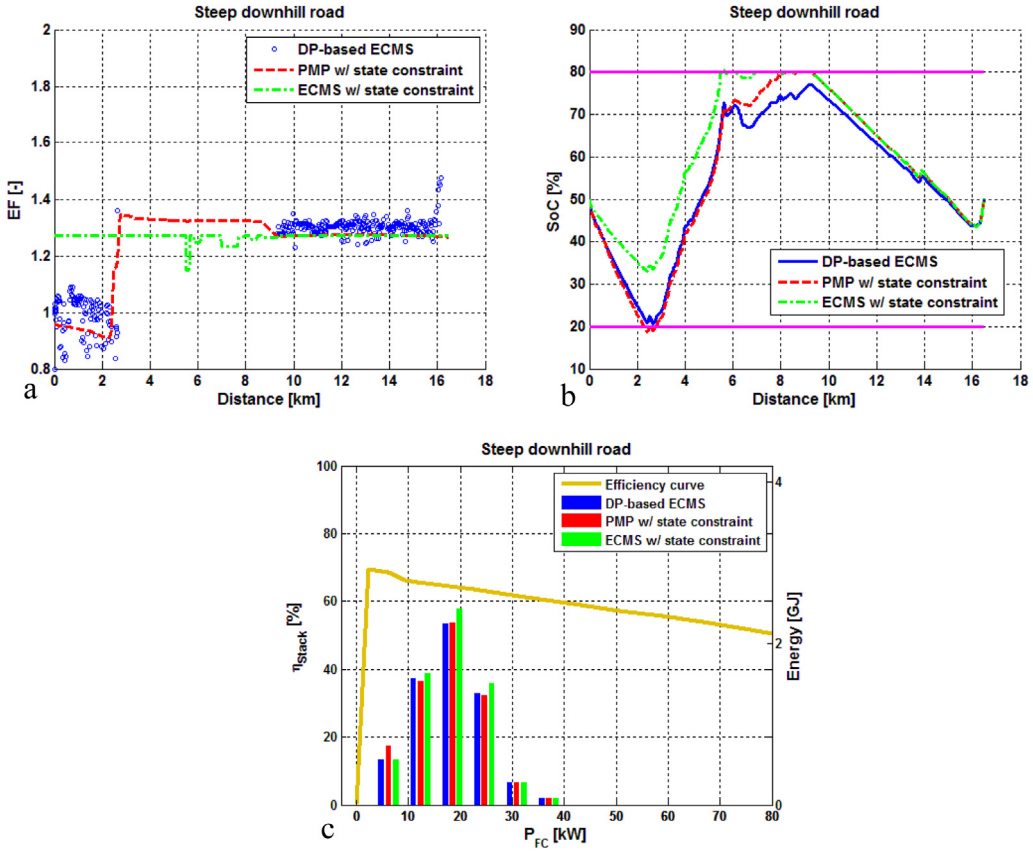

Fig. 6. Second steep downhill road for three EMSs (DP-based ECMS, PMP, conventional ECMS): (a) EF trajectory (b) battery SoC trajectory (c) energy histogram of fuel cell system.

(roughly −2.8°), and driver power demands for all hilly roads are shown in Fig. 9. Uphill road conditions are excluded in this paper because the effect of uphill information on fuel economy improvement is relatively small [28,29]. Fig. 10 shows that the optimal EF is held constant as long as the SoC boundary constraint is inactive. The value of constant EF, however, varies with the road grade. On the other hand, when steep downhill conditions activate the SoC constraint, EF must be adjusted for optimal fuel economy as well as charge-sustenance.

5.2.2. EF adaptation algorithm

Based on the analysis of DP-based EF trajectories, a real-time EF adaptation algorithm is proposed as follows. The proposed algorithm consists of two parts: static EF adaptation algorithm, dynamic EF adaptation algorithm. The static algorithm normally adjusts EF

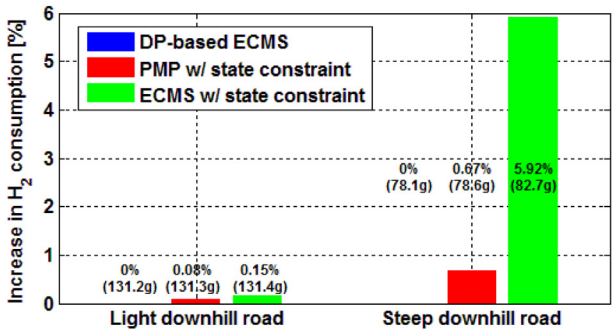

Fig. 7. Increase in H_2 mass consumption [%] compared to DP-based ECMS: final H_2 consumption of DP-based ECMS is considered reference to calculate increased amount of H_2 consumption of other EMSs under two hilly road conditions.

over light hilly road conditions, but the dynamic algorithm is activated when the state inequality constraints become active, which can be determined by the potential energy of the hilly road, i.e., when the potential energy exceeds the half of battery energy capacity. In order to determine whether potential energy exceeds the half of battery energy capacity, future driving information such as road slope profile and average velocity are necessary. This information enables the estimation of average power demand by using Eq. (6), and can be obtained from map database in Global Positioning System (GPS) navigation system.

A. Static EF adaptation algorithm

The static EF adaptation algorithm is developed based on an EF sensitivity analysis. Since the power demand varies under hilly road conditions due to gravitational force, a nominal EF designed for a flat road would lead to biases in battery power and SoC. Therefore, an EF adaptation algorithm is proposed to cancel out this battery power variation with respect to the power demand variation. Namely, one can find the EF variation that is necessary to cancel out the bias in optimal battery power due to the road grade from the following equality equation.

$$\Delta P^*_{\mathrm{BT\cdot req}}\Big|_{\Delta P_{\mathrm{demand}}} + \Delta P^*_{\mathrm{BT\cdot req}}\Big|_{\Delta s} = 0$$
$$\rightarrow \Delta s = -\left(\frac{\partial P^*_{\mathrm{BT\cdot req}}}{\partial P_{\mathrm{demand}}}\cdot \Delta \overline{P}_{\mathrm{demand}}\right) \Big/ \frac{\partial P^*_{\mathrm{BT\cdot req}}}{\partial s} \tag{34}$$

where $\Delta P^*_{\mathrm{BT\cdot req}}\Big|_{\Delta P_{\mathrm{demand}}}$ is the expected optimal battery power variation corresponding to the power demand variation, $\Delta P^*_{\mathrm{BT\cdot req}}\Big|_{\Delta s}$ is

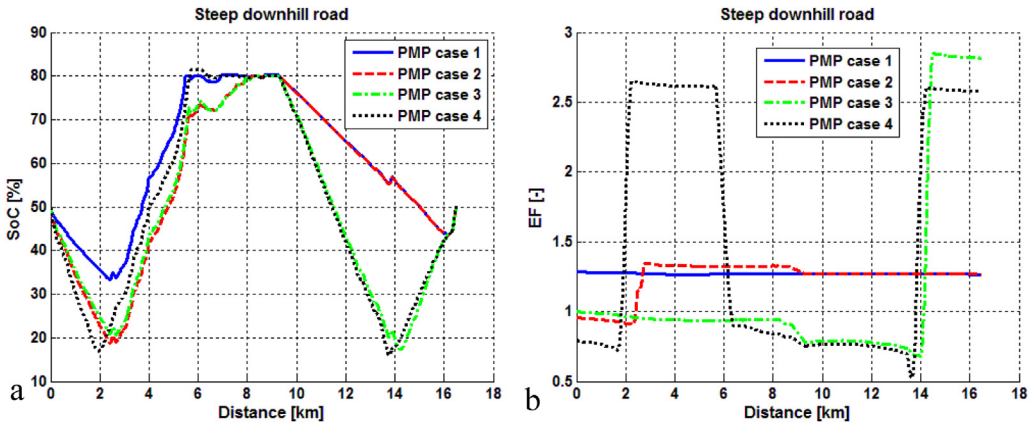

Fig. 8. Several PMP cases on second steep downhill road: (a) battery SoC trajectory, (b) EF (costate) trajectory.

Table 2
Initial costates and final H_2 mass consumption of PMP on second steep downhill road.

Second steep downhill road	PMP case 1	PMP case 2	PMP case 3	PMP case 4
$\lambda_1(t_0)$	0.0353	−0.0263	−0.0275	−0.0219
$\lambda_2(t_0)$	$-3.167e^{-4}$	−0.0498	−0.0796	−0.0526
H_2 mass [g]	82.7	78.6	88.3	95.0

the expected optimal battery power variation corresponding to the EF variation, $\partial P^*_{BT\cdot req}/\partial P_{demand}$ is the optimal battery power sensitivity to the power demand variation, $\partial P^*_{BT\cdot req}/\partial s$ is the optimal battery power sensitivity to the EF variation, and $\Delta\overline{P}_{demand}$ is the average power demand variation. Fig. 11(b) illustrates the sensitivity of the optimal EF with respect to the power demand variation. Herein, EF slope is determined by model parameters of fuel cell system and battery system. Readers are referred to [30] for more details.

B. Dynamic EF adaptation algorithm

The dynamic EF adaptation algorithm is designed based on the necessary condition for steep downhill road. In such case, the EF must be adjusted to compensate for the upcoming road grades because the potential energy is large enough to activate the state inequality constraints. For instance, the battery SoC should be depleted to minimum before arriving at the severely downhill section so that the battery can recharge the large potential energy as much as it can during the downhill section. After that, the maximum SoC should be depleted to desired SoC (initial SoC value) at destination. Therefore, each EF can be computed by solving Eq. (32). That is,

$$s \approx f(\overline{P}_{demand}, \overline{P}_{BT}) \quad \text{where } \overline{P}_{BT} = \frac{E_{BT\cdot lim}}{2}\cdot\frac{\overline{v}}{d} \tag{35}$$

where $\overline{P}_{demand}$ denotes the sectional average power demand, $\overline{P}_{BT}$ denotes the sectional desired battery power, $\overline{v}$ denotes sectional average velocity, $E_{BT\cdot lim}$ denotes battery energy capacity, and d denotes driving distance for each road section. Note that the future road grade is assumed known a priori in this study, and the road is divided into several sections by the road grade.

5.2.3. Performance evaluation: charge-sustenance and fuel economy

In this section, the charge-sustenance and fuel economy performance of the proposed EF adaptation strategy is evaluated via simulation. Three target hilly roads, light, medium, and steep downhill road, are employed for the evaluation. Note that only the steep downhill road has potential energy large enough to activate the SoC constraint, and the nominal EF is computed based on the flat road.

The fuel economies of three control strategies (DP-based EF, no EF adaptation, and proposed EF adaptation algorithm) are summarized for three levels of downhill road conditions in Fig. 12. Note that the fuel economy of each strategy is normalized by the DP fuel economy with the corresponding SoC for a fair comparison. As

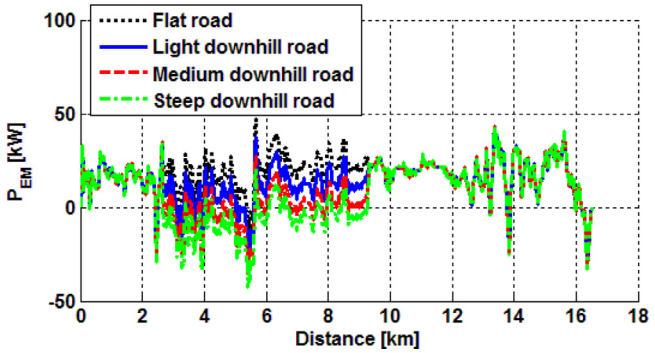

Fig. 9. Power demand profile: flat road, light downhill road, medium downhill road, and steep downhill road.

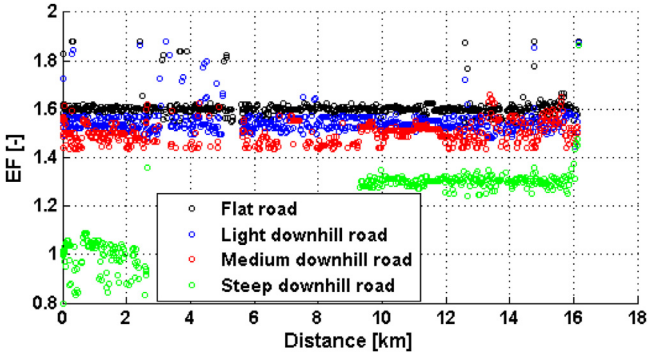

Fig. 10. DP-based EF trajectories for several hilly road conditions: flat road, light downhill road, medium downhill road, and steep downhill road.

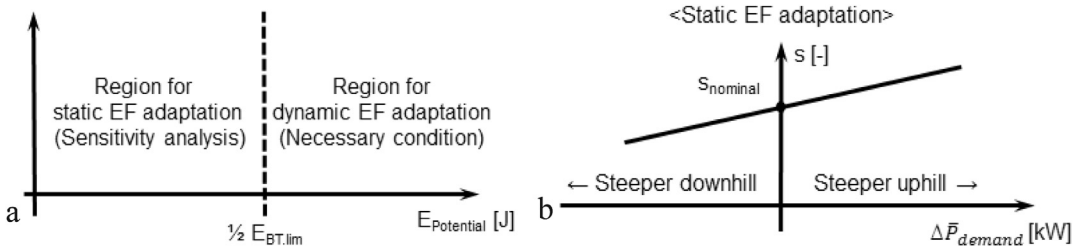

Fig. 11. (a) Classification of region for EF adaptation strategy (b) Static EF adaptation.

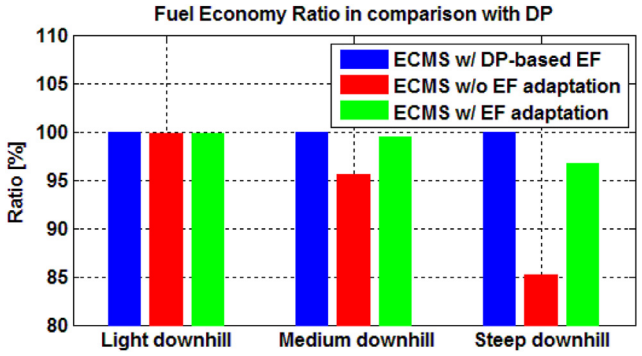

Fig. 12. Comparison of fuel economy performance: all fuel economy is normalized by DP fuel economy with the matching final SoC.

shown in Fig. 12, the proposed EF adaptation algorithm achieves near-DP fuel economy (less than 3% loss) while the ECMS without EF adaptation results in losses of fuel economy up to 15%. Fig. 13 illustrates that with increasing downhill road grade, both EF and SoC trajectories of the ECMS without EF adaptation start to deviate from those of the DP-based EF solution, which implies the loss of fuel economy and charge-sustenance. The loss of optimality is more pronounced for the steep downhill road case because the SoC constraint becomes active and the entire potential energy cannot be recuperated. The proposed EF adaptation algorithm, however, adjusts EF according to the road grade in order to compensate for the change in power demand as well as to prepare for the maximum recuperation of large potential energy available from the steep downhill road. These EF adjustments result in near-DP fuel

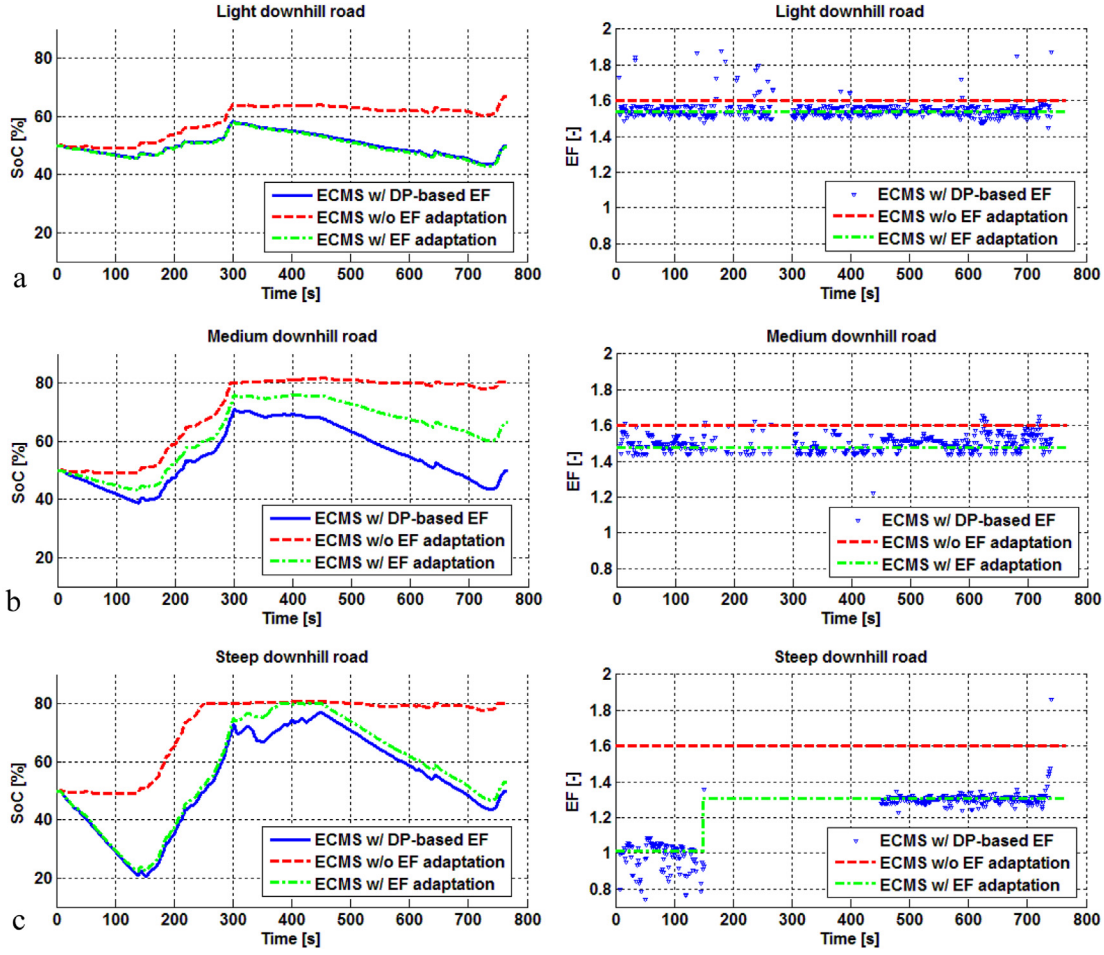

Fig. 13. Comparison of SoC and EF trajectories: (a) light downhill road, (b) medium downhill road, (c) steep downhill road.

economy and charge-sustenance performance for various hilly road conditions.

6. Conclusion

This paper proposes a method for extracting a globally optimal EF trajectory from the DP results as a benchmark for design of EF adaptation law. When the state inequality constraints are active, the DP-based ECMS approach has an advantage over the PMP approach because the latter yields multiple minimum solutions, and requires an iterative process to find the solution with the minimum cost. The extracted EF trajectory of DP-based ECMS represents the proper EF adjustment on hilly roads. A comparison of the DP-based ECMS' results with those of the PMP and the conventional ECMS shows that when hilly road conditions do not affect the SoC inequality constraints, the EF trajectories of all EMSs (DP-based ECMS, PMP, and conventional ECMS) are constant and almost the same. In contrast, when hilly road conditions activate the SoC inequality constraints, EF must be changed considerably for the optimal fuel economy; otherwise, the loss of optimality is significant. Therefore, the DP-based EF should provide useful insights and can be used to design an EF adaptation law as well as a benchmark. As an example, a real-time EF adaptation law is designed and evaluated over several hilly roads. Results show that it achieves superior fuel economy over the ECMS without EF adaptation. In fact, near-optimal performance was observed while maintaining the charge-sustenance. Future works include the improvement of the EF adaptation law for robust performance even with inaccurate future driving information.

Acknowledgments

This work was supported by the National Research Foundation of Korea (NRF) grant funded by the Korea Government (MSIP) (No. 2010-0028680), and the BK21 Program.

Appendix

Relationship between DP and PMP without constraints.

PMP can be derived from DP in continuous time in the case that there are no state constraints. Thus, this section deals with the interpretation of costate of PMP by analyzing of the relationship between DP and PMP. With DP, in continuous time, it is possible to obtain the sufficient condition by using the principle of optimality. This approach leads to a nonlinear partial differential equation by using the principle of optimality called the Hamilton–Jacobi–Bellman (HJB) equation [21], as follows:

$$-J_t^*(\mathbf{x},t) = \min_{\mathbf{u}\in U}\left\{g(\mathbf{x},\mathbf{u},t) + \left[J_x^*(\mathbf{x},t)\right]^T \mathbf{f}(\mathbf{x},\mathbf{u},t)\right\}$$

where $J^*(x(t),t)$ is the optimal cost-to-go function from time t to final time t_f. J_t^* and J_x^* are partial derivatives of $J^*(x(t),t)$ with respect to t and x.

The HJB equation is considered as both a necessary and a sufficient condition for optimality. The derivation of PMP from the HJB equation is given in Ref. [21]. In conclusion, the final formula obtained using the HJB equation is expressed under the condition that no state is not constrained by any boundary, as follows:

$$\frac{dJ_x^*(\mathbf{x}^*,t)}{dt} = -\left(\frac{\partial g(\mathbf{x}^*,\mathbf{u}^*,t)}{\partial \mathbf{x}}\right)^T - \left(\frac{\partial \mathbf{f}(\mathbf{x}^*,\mathbf{u}^*,t)}{\partial \mathbf{x}}\right)^T J_x^*(\mathbf{x}^*,t)$$

where the optimal control $u^*(t)$ satisfies

$$g(\mathbf{x}^*,\mathbf{u}^*,t) + \left[J_x^*(\mathbf{x}^*,t)\right]^T \mathbf{f}(\mathbf{x},\mathbf{u},t) = \min_{\mathbf{u}\in U}\left\{g(\mathbf{x}^*,\mathbf{u},t) + \left[J_x^*(\mathbf{x}^*,t)\right]^T \mathbf{f}(\mathbf{x}^*,\mathbf{u},t)\right\}$$

and the boundary condition

$$J_x^*\left(\mathbf{x}^*\left(t_f\right),t_f\right) = \left[\frac{\partial h}{\partial \mathbf{x}}\left(\mathbf{x}^*\left(t_f\right),t_f\right)\right]^T$$

As is evident from the above equation and boundary condition, J_x^* and the optimal costate λ^* of PMP satisfy the same differential equation and have the same boundary conditions; therefore, the optimal costate of PMP corresponds to the partial derivative of the optimal cost function with respect to x when the state constraints do not exist.

$$\boldsymbol{\lambda}^*(t) = J_x^*(\mathbf{x}^*,t)$$

This is assuming that the mixed partial derivatives are continuous.

References

[1] D. Feroldi, M. Serra, J. Riera, J. Power Sources 190 (2) (2008) 387–401.
[2] N.J. Schouten, M.A. Salman, N.A. Kheir, IEEE Trans. Contr. Syst. Technol. 10 (3) (2002) 460–468.
[3] J. Wu, C.-H. Zhang, N.-X. Cui, Int. J. Automot. Technol. 13 (7) (2012) 1159–1167.
[4] T. Hofman, M. Steinbuch, Int. J. Electr. Hybrid. Veh. 1 (1) (2007) 71–94.
[5] R.E. Bellman, Dynamic Programming, Princeton University Press, 1957.
[6] D.P. Bertsekas, Dynamic Programming and Optimal Control, Athena Scientific, Belmont, 2007.
[7] A. Brahma, Y. Guezennec, G. Rizzoni, in: Proc. of American Control Conference 2000, Chicago, USA, 28–30 June 2000, pp. 60–64.
[8] C. Lin, H. Peng, J.W. Grizzle, J. Kang, IEEE Trans. Contr. Syst. Technol. 11 (6) (2003) 839–849.
[9] G. Paganelli, G. Ercole, A. Brahma, Y. Guezennec, et al., JSAE Rev. 22 (4) (2001) 511–518.
[10] A. Sciarretta, M. Back, L. Guzzella, IEEE Trans. Contr. Syst. Technol. 12 (3) (2004) 352–363.
[11] P. Rodatz, G. Paganelli, A. Sciarretta, L. Guzzella, Contr. Eng. Pract. 13 (1) (2005) 41–53.
[12] J. Park, J.-H. Park, Int. J. Automot. Technol. 13 (5) (2012) 835–843.
[13] B. Gu, G. Rizzoni, in: Proceedings of ASME 2006 International Mechanical Engineering Congress and Exposition(IMECE), Chicago, USA, 5–10 November 2006, pp. 249–258.
[14] A. Chasse, P. Pognant-Gros, A. Sciarretta, SAE Int. J. Engines 2 (2009) 1630–1638.
[15] J. Kessels, M. Koot, P. van den Bosch, D. Kok, IEEE Trans. Veh. Technol. 57 (6) (2008) 3428–3440.
[16] D. Ambühl, L. Guzzella, IEEE Trans. Veh. Technol. 58 (9) (2009) 4730–4740.
[17] L. Serrao, S. Onori, G. Rizzoni, in: Proc. American Control Conference 2009, ST. Louis, USA, 10–12 June 2009, pp. 3964–3969.
[18] L. Serrao, S. Onori, G. Rizzoni, ASME J. Dyn. Syst. Meas. Contr. 133 (3) (2011).
[19] N. Kim, S. Cha, H. Peng, IEEE Trans. Contr. Syst. Technol. 19 (5) (2011) 1279–1287.
[20] N. Kim, A. Rousseau, D. Lee, J. Power Sources 196 (2011) 10380–10386.
[21] D.E. Kirk, Optimal Control Theory: An Introduction, Prentice Hall, New Jersey, 1970.
[22] L. Guzzella, A. Sciarretta, Vehicle Propulsion Systems, Springer, 2007.
[23] O. Sundström, L. Guzzella, in: Proc. 2009 IEEE Multi-Conference on System and Control, Saint Petersburg, Russia, 8–10 July, 2009, pp. 1625–1630.
[24] C. Lin, H. Peng, J.W. Grezzle, J. Liu, M. Busdiecker, SAE Technical Paper, 2003-01-3369.
[25] Y. Zhu, Y. Chen, G. Tian, H. Wu, Q. Chen, in: Proc. 2004 American Control Conference, Boston, USA, 30 June–2 July 2004, pp. 156–161.
[26] D. Kum, H. Peng, N.K. Bucknor, ASME Trans. Dyn. Syst. Meas. Contr. 133 (6) (2011).
[27] D. Kum, H. Peng, N.K. Bucknor, IEEE Trans. Contr. Syst. Technol. 21 (1) (2013) 14–26.
[28] J. Han, D. Kum, Y. Park, Int. J. Automot. Technol. 15 (2014) 1–8.
[29] C. Zhang, A. Vahidi, P. Pisu, X. Li, K. Tennant, IEEE Trans. Veh. Technol. 59 (3) (2010) 1139–1147.
[30] J. Han, Y. Park, D. Kum, S. Ryu, SAE Int. J. Alt. Power 3 (1) (2014) 72–77.